Journal of Archaeological Science 40 (2013) 2686–2701

Contents lists available at SciVerse ScienceDirect

Journal of Archaeological Science

journal homepage: http://www.elsevier.com/locate/jas

Archaeological and archaeomagnetic dating at a site from the *ager Tarraconensis* (Tarragona, Spain): El Vila-sec Roman pottery

Marta Prevosti [a], Lluís Casas [b,*], Josep Francesc Roig Pérez [c], Boutheina Fouzai [d], Aureli Álvarez [b], Àfrica Pitarch [e]

[a] Institut Català d'Arqueologia Clàssica, Plaça d'en Rovellat, s/n, 43003 Tarragona, Catalonia, Spain
[b] Universitat Autònoma de Barcelona, Facultat de Ciències, Departament de Geologia, Campus de la UAB, 08193 Bellaterra, Catalonia, Spain
[c] CODEX Arqueologia i Patrimoni, Pl. Sant Fructuós 1, 43002 Tarragona, Catalonia, Spain
[d] Université de Tunis El Manar, Faculté des Sciences, Département de Géologie, Campus Universitaire, 2092 Manar II, Tunisia
[e] IBeA Research Group, Department of Analytical Chemistry, Faculty of Science and Technology, University of the Basque Country (UPV/EHU), Barrio Sarriena s/n, 48940 Leioa, Bizkaia, Spain

ARTICLE INFO

Article history:
Received 1 August 2012
Received in revised form
11 January 2013
Accepted 24 January 2013

Keywords:
Archaeomagnetism
Ceramic
Typology
Dating
Geomagnetic field modelling
Archaeodirection
Archaeointensity

ABSTRACT

A very accurate archaeological dating of a Roman site in NE Spain (El Vila-sec) was made based on the typology of pottery artifacts. Three different phases were identified with activity ranging from the mid-1st century BC to the early-3rd century AD. Analyses of bricks from kilns at El Vila-sec produced data on their stored archaeomagnetic vector. These data were compared with the secular variation curve for the Iberian Peninsula and the SCHA.DIF.3K regional archaeomagnetic model. Both, the reference curve and the model, produced probability distributions for the final period of use for two kilns from the second archaeological phase that were not used during the third phase. At a 95% confidence level, both time distributions cover a wide chronological range including the presumed archaeological age. Both the Iberian secular variation curve and the SCHA.DIF.3K regional model proved to be suitable models for dating the site, although on their own they do not produce a single unambiguous solution. This archaeomagnetic approach could also be applied to neighbouring archaeological sites that have an imprecise archaeological age.

1. Introduction

Since the appearance of archaeomagnetism as a dating tool for archaeological sites (Aitken, 1974), such dating has been based on the use of secular variation curves (SVC) (e.g. Le Goff et al., 2002; Gómez-Paccard et al., 2006; Zananiri et al., 2007). These reference curves are arbitrarily centred on a given location and involve the relocation of data from sites that are both well-dated (to built the SVC) and poorly-dated (to attempt archaeomagnetic dating) sites. The relocation of archaeomagnetic data to a central location is a procedure that involves an inherent error (Casas and Incoronato, 2007). The current trend in archaeomagnetic dating tools is to develop geomagnetic models of the secular variation that can be used to obtain an ad hoc SVC for the specific site we are interested in. Despite this, the reliability of these models depends largely on the availability of experimental data close to the area and time under study (Casas et al., 2008). Consequently, archaeomagnetic dating of sites from areas with a limited record of well-dated sites appears to be somewhat imprecise and, in particular with regard to archaeomagnetic intensities, large discrepancies can be found between model predictions and actual data determinations (Fouzai et al., 2012; Schnepp et al., 2009). In contrast, in countries with an extensive archaeomagnetic record, the models tend to agree with the measured data (e.g. Catanzariti et al., 2012). Dating is thus possible and in some cases the obtained ages can constrain the presumed ones derived from archaeological evidence (Gómez-Paccard and Beamud, 2008).

In this paper we present the results from excavations at El Vila-Sec pottery (NE Spain). The site comprises twelve kilns and the finds made inside them allow a very precise identification of when they were abandoned. Archaeomagnetic dating has been attempted for some of these kilns to verify the accuracy of archaeomagnetic dating tools in NE Spain and to provide new archaeomagnetic data from well-dated archaeological features.

* Corresponding author. Tel.: +34 935868365; fax: +34 935811263.
E-mail address: Lluis.Casas@uab.cat (Ll. Casas).

0305-4403/$ – see front matter © 2013 Elsevier Ltd. All rights reserved.
http://dx.doi.org/10.1016/j.jas.2013.01.027

2. El Vila-sec pottery

2.1. Archaeological framework

El Vila-sec is an extraordinary archaeological site in the *Tarraco ager*, due to the number of excavated and datable kilns, as well as the variety of pottery produced there, including Dressel (Dr.) 2–4 amphorae (Dressel, 1899a; Sciallano and Sibella, 1993; López Mullor and Martín, 2008), Hispanic *terra sigillata*, thin-walled ware and oil lamps. The coastal strip of the *Hispania Tarraconensis* province was an area famous for its wine in antiquity (López Mullor and Aquilué, 2008; Prevosti and Martín i Oliveras, 2009). Amphorae for wine bottling were manufactured at several potteries which also produced building materials, coarse ware, *terra sigillata* and sometimes even other types of fine ware. It is vital to know how these potteries evolved in order to trace the development of economic life in Roman times and particularly in the *Camp de Tarragona* area, where such workshops are frequent and of a considerable size (Prevosti and Guitart i Duran, 2010, 2011).

A well-checked final dating for the wine amphorae from Tarragona is of great archaeological interest, as it is crucial to know the chronological periods of such an important economic activity as the trade in Tarragona wine in Roman times (Járrega and Otiña, 2008; Berni Millet, 2010, 2011; Járrega and Prevosti, 2011), which is mentioned in classical sources (Prevosti, 2009).

2.2. The archaeological site, excavations and archaeological dating

The widening of the C-14 highway between the towns of Alcover and Reus in 2006 and 2007 allowed the existence of a pottery (*figlina*) with a total surface area of around 2300 m^2 to be confirmed in the area of Vila-sec (near Alcover). Roig (2009, 2010) documented twelve kilns and numbered them from 1 to 12 (Fig. 1), a numbering we use in this article. El Vila-sec is one of the largest Roman potteries discovered in the province of *Hispania Tarraconensis*.

Roig's (2007, 2008, 2009, 2010) archaelogical excavations helped to identify two different zones with pottery kilns and to distinguish three chronological phases. In addition to the twelve kilns, other parts of the site were also excavated, including six settling basins for the clay, a kneading trough, *tegulae* channels, a large store and some areas used to process, shape and dry pottery items. The production from this industrial workshop consisted of tableware, cooking ware, thin-walled ware, architectural pottery, *doliae*, Hispanic *terra sigillata*, probably lamps and especially amphorae of the Dr. 2–4 and late Dr. 2–4 types.

The first identified phase of activity at the pottery consists of seven kilns (1–7 in Fig. 1). No pottery associated with the construction of these kilns was found as the construction trenches were dug directly into the geological substratum. However, their stratigraphic position dates them to prior to the second identified phase (mid-1st century AD).

The pottery produced during this first phase consisted of building materials (*tegulae*, *imbrex* and *antefixes*), *pondera*, coarse ware (especially plates, casseroles, bowls, bottles, jars, mortars, basins and lids), lamps, Hispanic *terra sigillata* and especially thin-walled ware. The Hispanic *terra sigilata* ceramics includes (Fig. 2) imitations of South Gaulish *terra sigillata* goblets of the forms Dragendorff (Drag.) 24/25b and Drag. 27b (Dragendorff, 1895; Ritterling, 1913; Oswald and Pryce, 1920; Mezquíriz, 1961, 1985; Passelac and Vernhet, 1993; Roca and Fernández García, 2005; Genin, 2007). The thin-walled ware includes (Fig. 3) Mayet 18 (10 BC to 60–70 AD), Mayet 21 (period of Augustus), Mayet 29 (period of Tiberius), Mayet 30 (period of Tiberius), Mayet 33 (period from Augustus to Claudius), Mayet 35 (period from Tiberius to Nero),

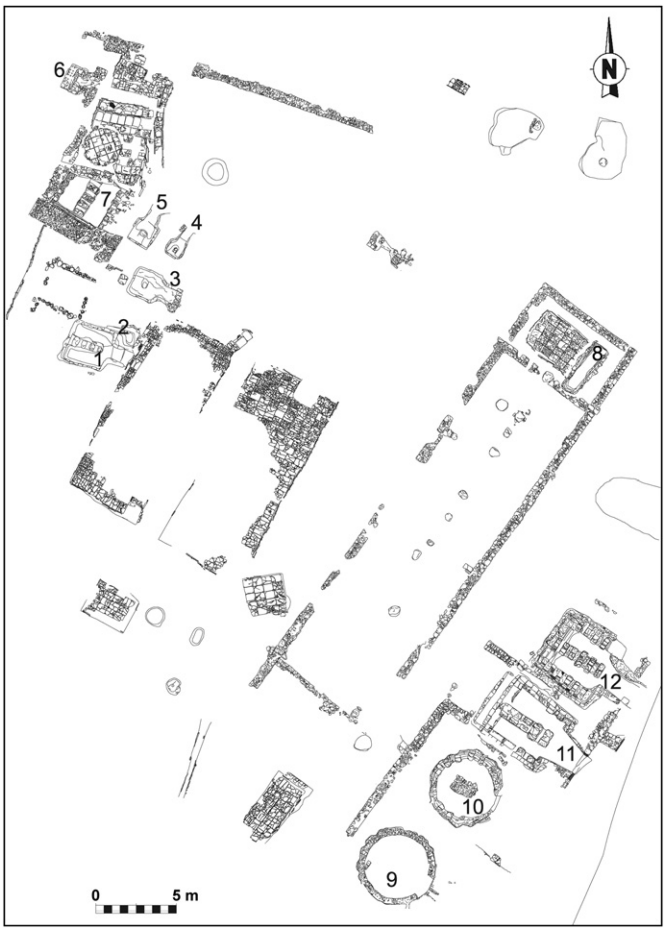

Fig. 1. General plan of El Vila-sec pottery; the kilns are numbered as in Roig (2009).

Mayet 36 (period from Tiberius to Nero), Mayet 37 (period from Tiberius to Nero), Mayet 38 (30–35 AD to 75–80 AD) and López 54 (20 BC–50 AD) (Mayet, 1975; López Mullor, 1989), as well as other unclassified shapes that are identifiable as beakers or bowls. An early small-scale production of Dr. 2–4 amphorae associated with Kiln 7 (Fig. 1) was also reported. The first phase can therefore be dated to between the Augustan era and the middle of the 1st century AD.

The second phase is characterized by the abandonment of all the preceding kilns and the construction of a second group of four kilns built in a line (Kilns 9–12, Fig. 1). These were located at the south-eastern end of the site and there was also a series of structures related to the production and storage of finished pieces. The construction of the kilns can be dated to the middle of the 1st century AD, based on strata from the destruction of the previous kilns and the levelling of the ground to prepare it for the new building works. It is worth to mentioning the materials that characterize these strata: i) Italic *terra sigillata* Conspectus (Consp.) 18.2 (15 BC–30 AD), Consp. 23.1 (25–75 AD), Consp. 33.1 (1–50 AD) and Consp. 36.3.2 (10–30 AD) (Ettlinger et al., 1990) forms; ii) South Gaulish *terra sigillata* Drag. 15a1 (1–60 AD), Drag. 15b1 (60–120 AD), Drag. 17b (25–60 AD), Drag. 18a (15–60 AD), Drag. 24/25b (40–70 AD), Drag. 27b (40–80 AD), Drag. 33a1 (20–60 AD), Haltern 5 (10–50 AD) and Ritterling 12 (40–70 AD) (Dragendorff, 1895; Ritterling, 1913; Oswald and Pryce, 1920; Passelac and Vernhet, 1993; Genin, 2007) forms; iii) African coarse ware Ostia II, 306 (14–117 AD) (Berti et al., 1970; Hayes, 1972) form; iv) thin-walled ware Mayet 21 (25 BC–25 AD), Mayet 30 (10–50 AD), Mayet 33 (10–30 AD), Mayet

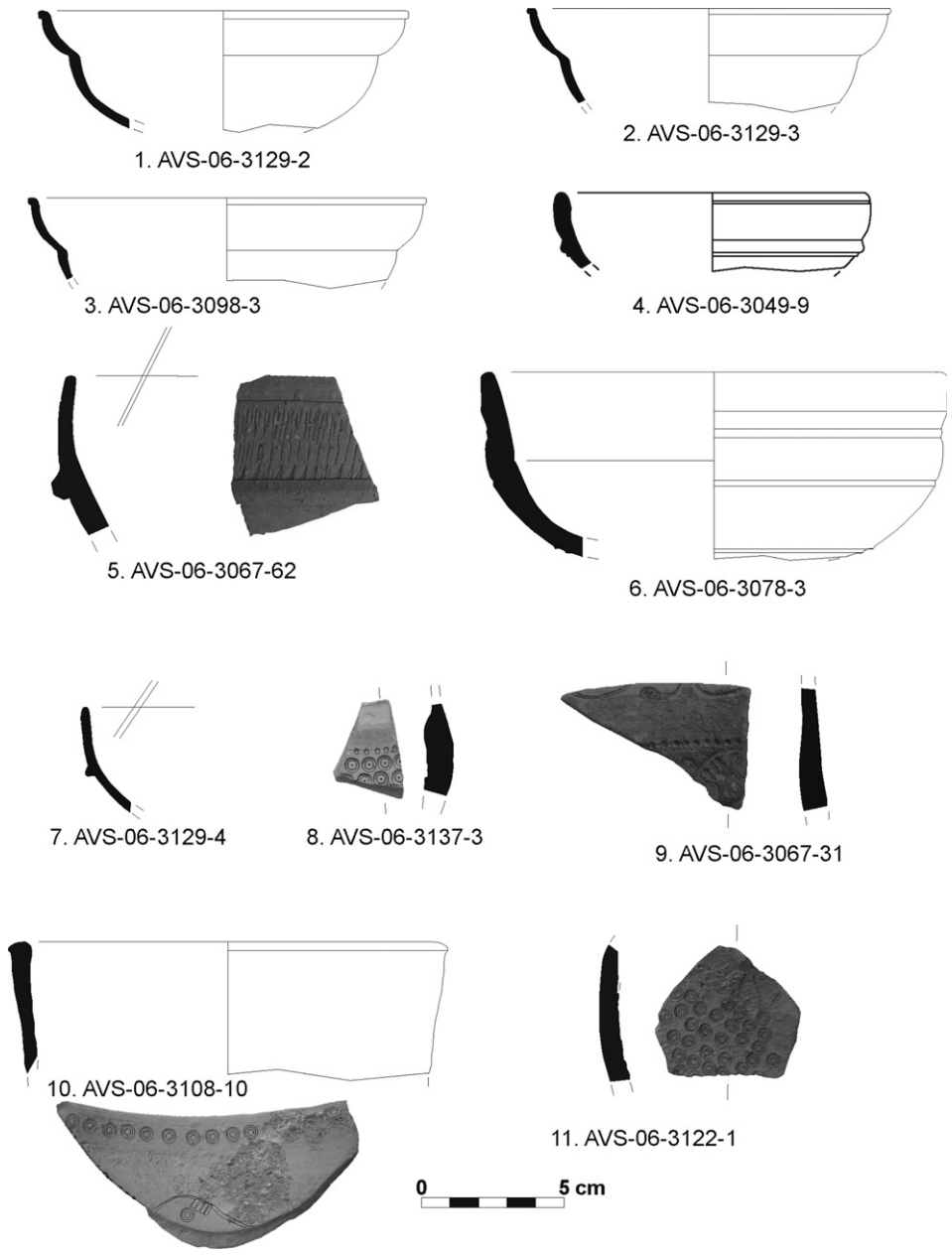

Fig. 2. Hispanic *terra sigillata* made at El Vila-sec during the first phase (1–3, Drag. 27; 4–7, Drag. 24/25; 8–11, moulds). The inventory numbers correspond to Roig (2010). Due to the high degree of erosion of fragments 5 and 8–11, the negatives of decorative motifs have been highlighted to make them easier to observe.

35 (15–60 AD), Mayet 37 (25–60 AD) and López 54 (20 BC–50 AD) (Mayet, 1975; López Mullor, 1989) forms; v) Amphorae, particularly from southern Hispania, i.e. Dr. 7–11 (25 BC–100 AD), Dr. 20B (30–50 AD) and Haltern 70 (50 BC–75 AD) forms, and among those produced in Tarragona, Oberaden 74 (1–30 AD), Pascual 1 (50 BC–50 AD) and the ever-present Dr. 2–4 (25 BC–300 AD) (Pascual, 1977; Sciallano and Sibella, 1993; Raynaud, 1993a; López Mullor and Martín, 2008); vi) also of note is a volute lamp, type Dr. 9B (Claudian era) (Dressel, 1899b; Pavolini, 1987; Morillo Cerdán, 1989); and lastly a dupondius from Tiberian period (21/22–37 AD).

The pottery manufactured during this second phase is clearly made up of Dr. 2–4 amphorae and, to a lesser extent, building material (*tegulae* and *imbrex*) and coarse ware (storage pots, cooking pots, casseroles and small jars) (Fig. 4).

The third phase of activity at the pottery is indicated by a series of small alterations and functional changes visible at different points of the site. These especially concern the construction of Kiln 8 (Fig. 1) and alterations carried out on Kilns 11 and 12 (Fig. 1) from the second phase. Dating of the third phase is based on a soil level, that corresponds to the backfill level of Stratigraphic Unit 3092 (Roig, 2010), which is related to the construction of an area delimited by rows of late Dr. 2–4 amphorae placed top downwards (Fig. 5). These amphorae date from the 2nd century and the first half of the 3rd century AD (Járrega and Otiña, 2008). Within this level, a number of pottery items was recovered reinforcing the dating of this phase to the 2nd century AD: Hispanic *terra sigillata* type Drag. 15/17 (30–300 AD), Drag. 37a (70–300 AD) and Drag. 37b (70–100 AD) (Mezquíriz, 1961, 1985; Roca and Fernández García, 2005).

This third phase is associated with the production of late or evolved Dr. 2–4 amphorae, although some manufacture of building materials and coarse ware cannot be excluded. In fact, the kilns

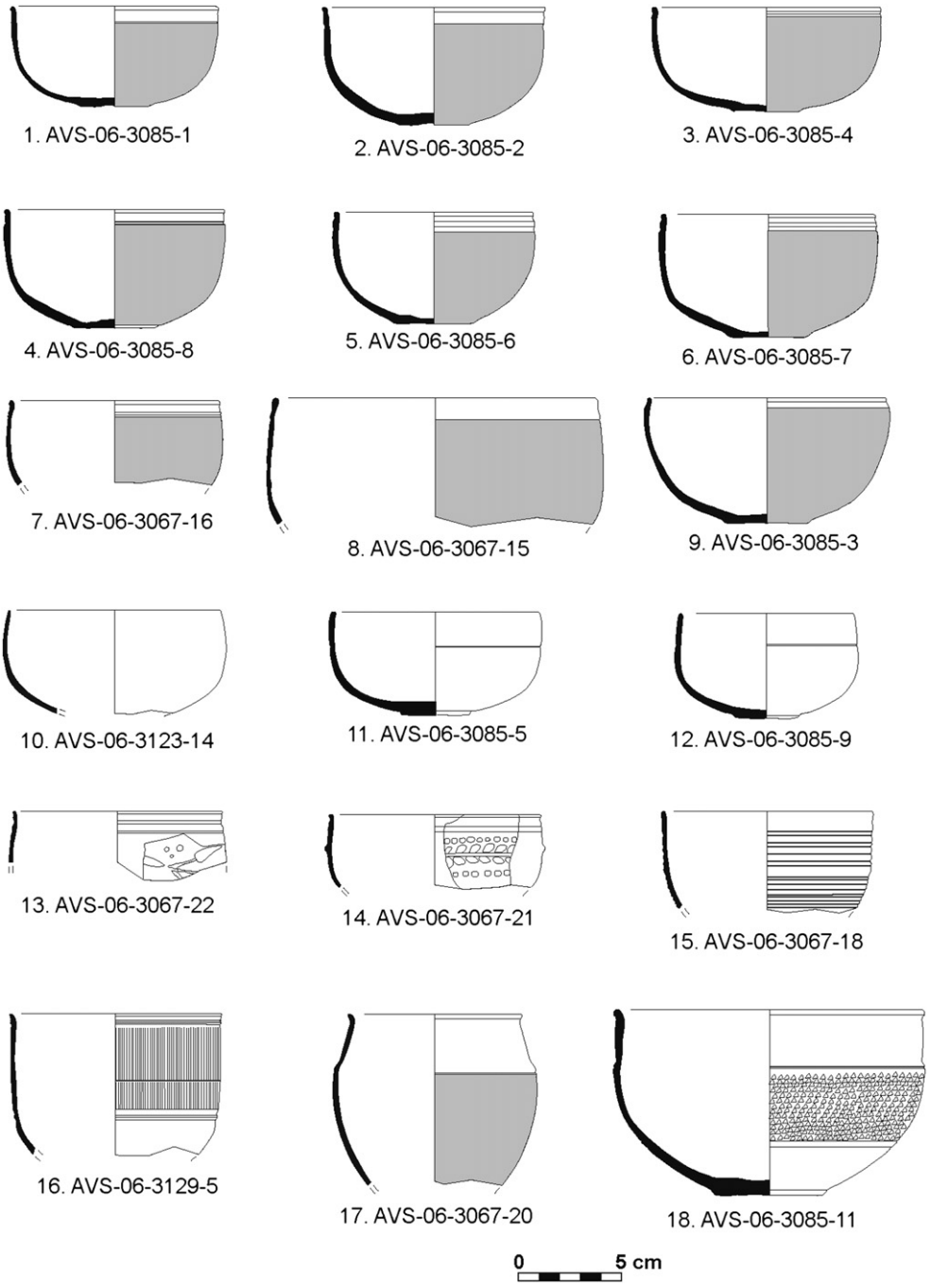

Fig. 3. Thin-walled ware made at El Vila-sec during the first phase (1–4, Mayet 37 form; 5–8, Mayet 30 form; 9 and 10, Mayet 35 form; 11–12, Mayet 33 form; 13 and 14 Mayet 29 form; 15, original bowl from El Vila-sec; 16 original beaker from El Vila-sec; 17, Mayet 21 form: 18, López 54 form). The inventory numbers correspond to Roig (2010).

from this phase are either too small (Kiln 8) for firing amphorae or they have evidence of direct firing (Kilns 11 and 12) and therefore amphorae would have been produced in Kilns 9 and 10.

This hypothesis cannot be confirmed until the completion of the pending excavations.

The pottery structures were in filled and abandoned in the late 2nd or early 3rd centuries AD. The materials that allow the dating of the uppermost strata are: i) African Red Slip (ARS) ware *terra sigillata* chiara A: Lamboglia (Lamb.) 2a (100–175 AD) and Lamb. 4/36A (90–175 AD) forms and ARS coarse ware; among the finds are worthy of mention are: Lamb. 10A (100–450 AD), Lamb. 10B (69–250 AD), Ostia III, 267A (100–475 AD) and Ostia III, 324 (100–300 AD) pots and the lid of an Ostia III, 332 type pot (69–450 AD) (Lamboglia, 1958; Berti et al., 1970; Hayes, 1972; Raynaud, 1993b,c); ii) Hispanic *terra sigillata*, with of particular note the Drag. 15/17 (30–300 AD), Drag. 18 (50–200 AD), Drag. 24/25 (30–150 AD), Drag. 30 (50–100 AD), Drag. 35 (50–150 AD) and Drag. 36 (50–300 AD), Drag. 37a (70–300 AD) and Drag. 37b (70–100 AD) (Mezquíriz, 1961, 1985; Roca and Fernández García, 2005) forms. This collection of pottery dates the abandonment of the structures to the end of the 2nd century AD, although the find of an extremely eroded Antoninian coin dated to the 3rd century AD extends the duration of the final fill of the pottery workshop remains into the next century.

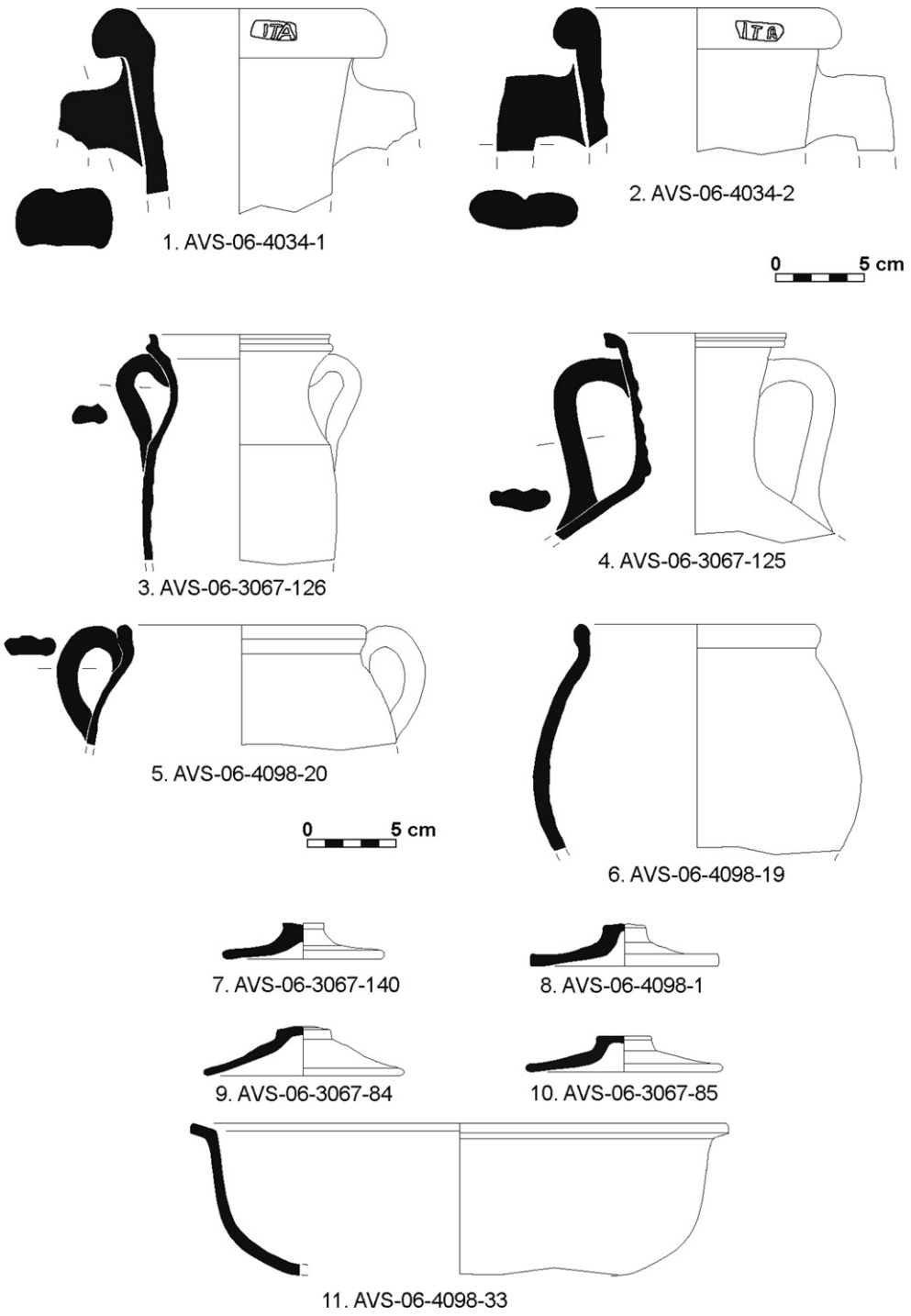

Fig. 4. Pottery made at El Vila-sec during the second phase (1 and 2, amphorae Dr. 2–4 with the stamp ITA; 3 and 4, jars; 5 and 6, pots; 7–10, covers; 11: casserole). The inventory numbers correspond to Roig (2010).

In summary, we can state that the first phase (including Kilns 1–7) can be dated to the time of Augustus and that they were rendered inoperative by the building of the second occupation phase (which includes Kilns 9–12) from the mid-1st century AD. It should be noted that excavation of Kilns 9 and 10 could not be completed and their chronological evolution is therefore not known. However, Kilns 11 and 12 were fully excavated and therefore it is known that they were altered in the mid-2nd century AD, within what we call the third phase. It was also at this time that Channel-Kiln 8 was built. All five kilns (second and third phases of occupation) were definitively filled in during the late 2nd - early 3rd centuries AD.

2.3. Detailed description of the sampled kilns

Unfortunately, the remaining kiln structures from the first building phase were quite damaged. The walls of their combustion chambers were eroded and crumbling and thus not easily

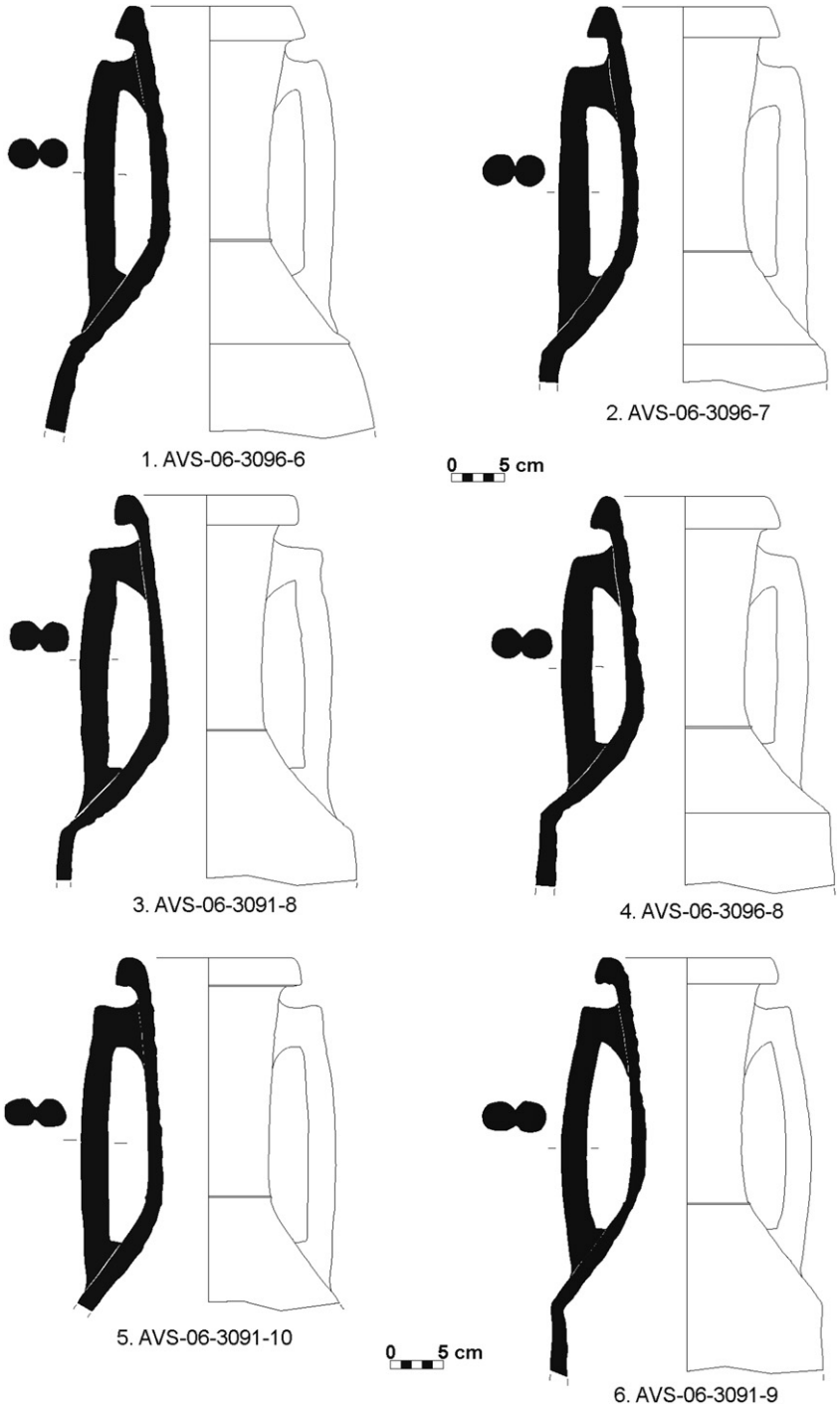

Fig. 5. Late Dr. 2–4 amphorae made at El Vila-sec during the third phase. The inventory numbers correspond to Roig (2010).

samplable for archaeomagnetic purposes. Only Kiln 7 (Fig. 6) was successfully sampled.

The structure of Kiln 7 was partly destroyed by later building phases, so it was not possible to delimit the *praefurnium*, although it is recognizable that the access to this opening was via its northern side. An axial wall that divides the chamber lengthwise into two was preserved within the firing chamber. The remains of five arches were also visible; they supported the clay pipe grid, which was not preserved. This kiln can be included within Cuomo di Caprio's Type II/c (rectangular with a double passageway) (Cuomo di Caprio, 1971–1972, 1985, 2007). Three loose and quite crumbly quadrangular bricks from the base of the arches from Kiln 7 were removed and drilled in the laboratory, and finally cut to produce 23 standard cylindrical (~2.5 cm diameter) specimens for archaeointensity determinations.

Three of the four kilns built in the second building phase were sampled. These are Kilns 9 (Fig. 7), 11 (Fig. 8) and 12 (Fig. 9). Kiln 9 is circular with a diameter of about 3 m. There is a perimeter stone and mud wall and an inner *latericium* or brick wall of the firing chamber. As the excavation could not be completed, an accurate

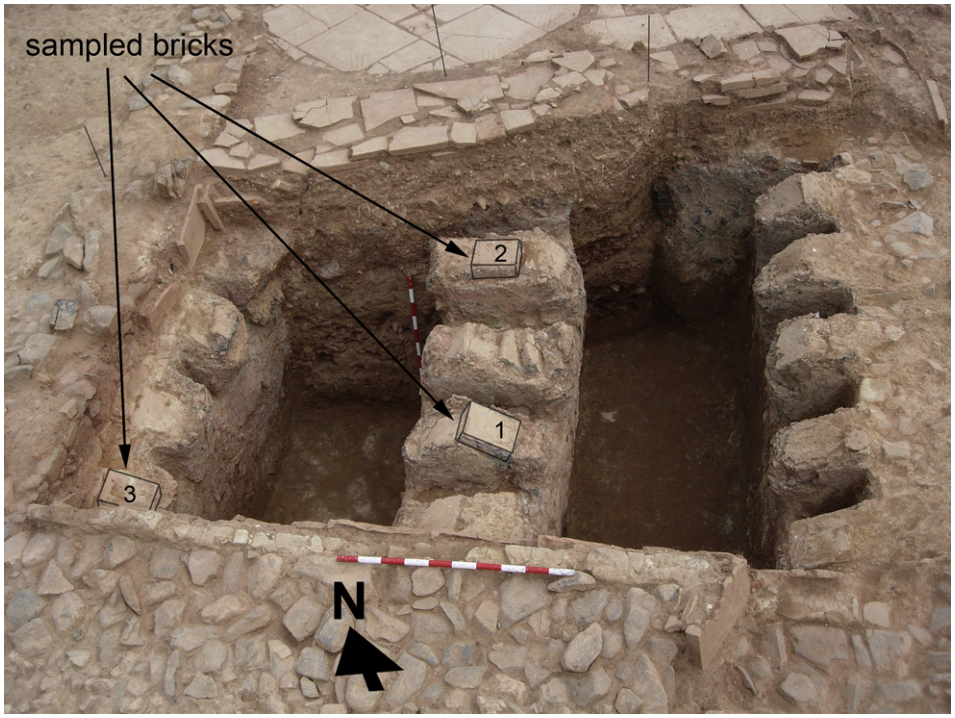

Fig. 6. Kiln 7 with indication of the sampled bricks. This kiln produced Dressel 2–4 amphorae between the Augustan era and the middle of the 1st century AD. The rectangular structure with a double passageway corresponds to *N*. Cuomo di Caprio's (1971–1972, 1985, 2007) Type II/c.

classification cannot be made, although it may be Type I/b (circular with a clay pipe grid supported by a radial wall) from Cuomo di Caprio's (1971–1972, 1985, 2007) classification. Kilns 11 and 12 are rectangular; the preserved parts are those excavated in the substratum i.e. the firing chamber and the *praefurnium*. A perimeter wall and an axial inner wall were reported for both. The perimeter walls are made of mud bricks, bricks and fragments of *tegulae* bound with mud, whereas the axial walls of the firing chamber are made of bricks bound with mud. Similarly to Kiln 7, on the three walls that delimit the firing chamber of these kilns there are the

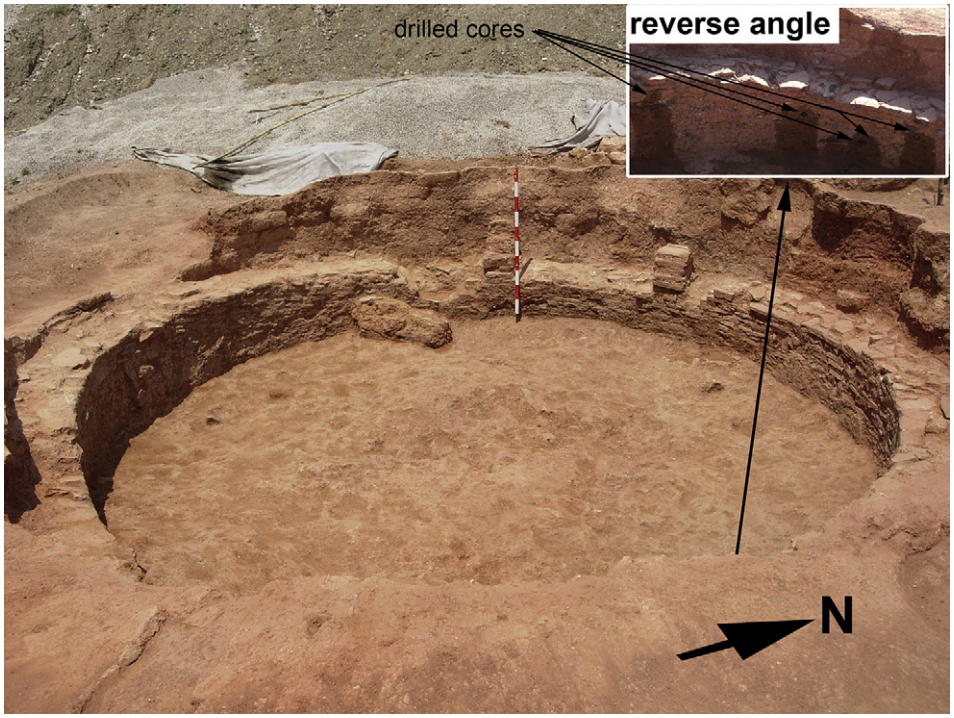

Fig. 7. Kiln 9 with indication of the drilled cores. This kiln has a perimeter mud stone wall and an inner firing chamber wall made of latericium or brick material. It is probably an *N*. Cuomo di Caprio (1971–1972, 1985, 2007) Type I/b.

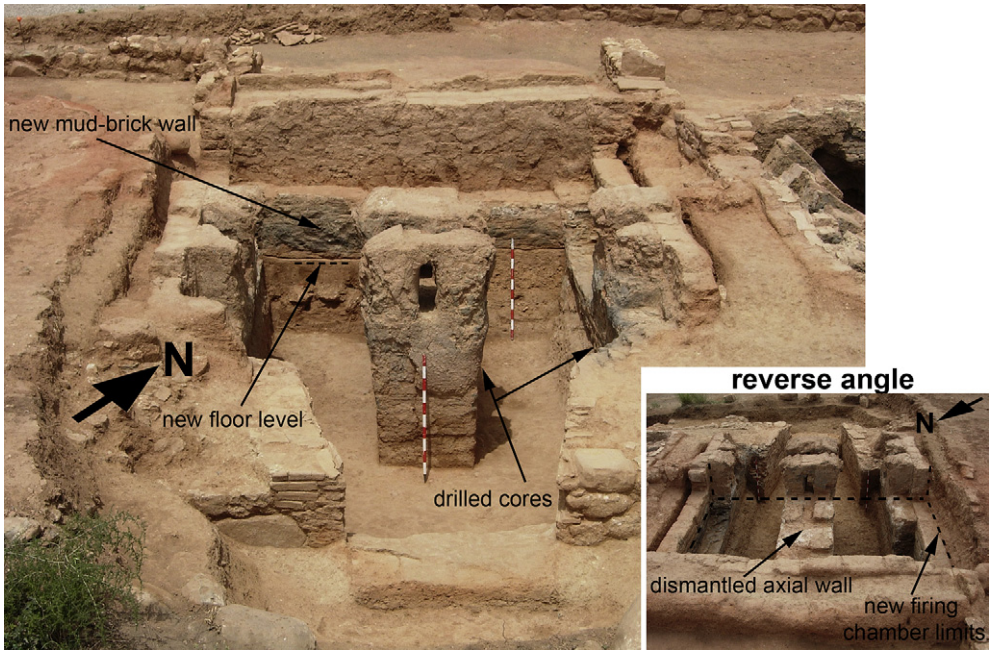

Fig. 8. Kiln 11 with indication of the sampled areas and late restructuring features. This kiln was built during the second phase and rebuilt in the middle of the 2nd century AD. The original rectangular structure with a double passageway corresponds to *N.* Cuomo di Caprio's (1971–1972, 1985, 2007) Type II/c.

remains of the arches that supported the clay pipe grid, which again was not preserved. In the case of Kiln 12, a ventilation hole or air flue was reported in the western corner. According to the Cuomo di Caprio's (1971–1972, 1985, 2007) classification both kilns also correspond to Type II/c (rectangular with double passageway). Kils 11 and 12 were restructured during the third building phase. Kiln 11 was made smaller, using the firing chamber from the previous phase. At the rear, the upper part of the axial wall was dismantled, a new mud-brick wall on its north-western side was built and the firing chamber floor level was raised (Fig. 8). The result is a smaller kiln with two openings on all sides of the earlier axial wall. Kiln 12 underwent a similar reorganization (Fig. 9): the eastern corner of

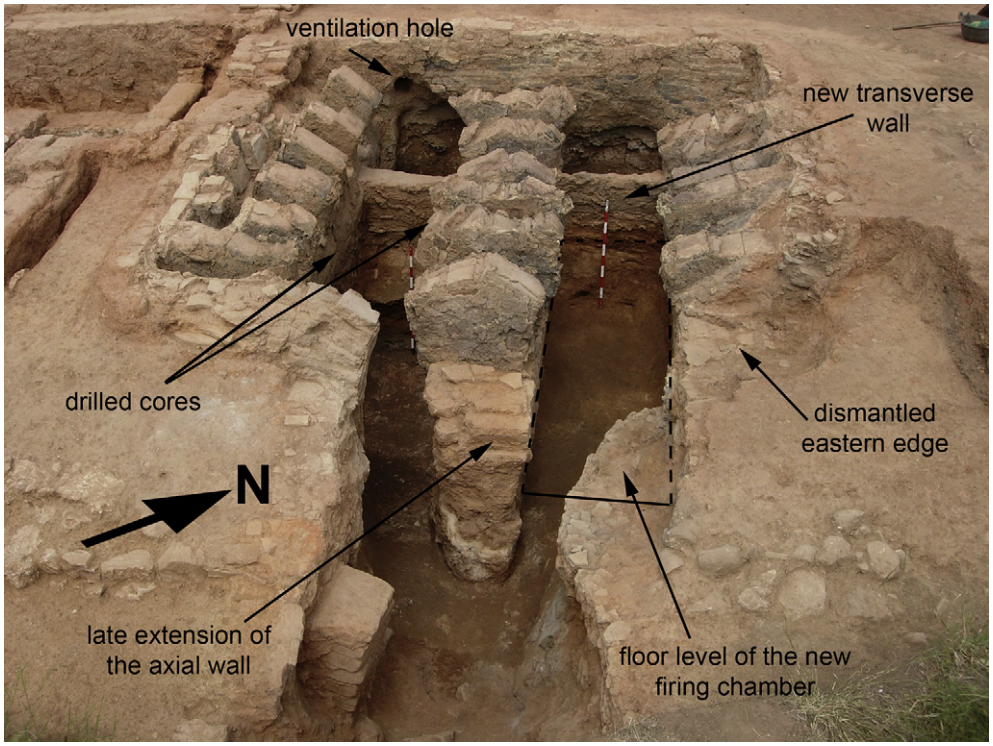

Fig. 9. Kiln 12 with indication of the sampled areas, the ventilation hole and late restructuring features. Like Kiln 11, it was build during the second phase and rebuilt in the middle of the 2nd century AD. The original rectangular structure with a double passageway corresponds *N.* Cuomo di Caprio's (1971–1972, 1985, 2007) Type II/c.

the perimeter wall of the previous firing chamber was dismantled, a new transverse wall was built to move the firing chamber forward, lengthening the axial wall with an extension made of bricks and mud bricks bound with mud, and the floor level of the chamber was raised. The result was that the firing was concentrated between the old axial wall and the earlier north-eastern wall whereas the gap between the earlier axial wall and the earlier south-western wall was abandoned and filled with earth. With the current available data, it is not possible to determine whether the restructured kilns (11 and 12) were still used to fire pottery or another kind of material.

Oriented samples were retrieved from the internal *opus latericium* walls of Kilns 9 (Fig. 7), 11 and 12 for archaeodirectional determinations. For Kilns 11 and 12, sampling was performed on structures not fired during the third archaeological phase: the abandoned firing chamber below the new floor level (Fig. 8) and the abandoned south-western passageway (Fig. 9). A portable electrical drill with a water-cooled diamond bit was used following the standard palaeomagnetic sampling procedure; each core produced a single specimen. The in situ azimuth and dip of the cores were measured using a compass coupled to a core-orienting fixture. Due to the crumbly consistency of the walls, drilling had to proceed delicately to avoid breaking the cylinder before taking its orientation. If broken, the cylinder was carefully placed back in its hole to mark its orientation. From three rejected, misoriented cylinders from Kiln 12 (the first sampled), small cylinders (5 mm diameter, 3 mm length) were sub-sampled in the laboratory for microwave archaeointensity determinations. Samples from Kilns 11 and 12 had the most constrained archaeological age as they correspond to structures fired during the second archaeological phase (mid 1st century AD-mid 2nd century AD), but not during the third one. In contrast Kiln 9 could actually have continued to operate during the third archaeological phase.

To sum up, 62 specimens were obtained from 4 kilns at the Vilasec Roman pottery with a very precise archaeological age. Table 1 summarizes the details of all the sampled structures, their presumed archaeological ages and the number of samples taken.

3. Experimental methods and data analyses

Rock magnetic properties were measured at the Geomagnetism Laboratory, University of Liverpool for core samples from Kiln 7 and for several rejected misoriented cores from Kiln 12. Plate-like samples were cut from the cores and their change in susceptibility was measured as they warmed from liquid nitrogen to room temperature. Hysteresis properties, isothermal remanent magnetization (IRM) acquisition, remanence coercivity and magnetization versus temperature curves were obtained by using a Magnetic Measurements variable field translation balance (VFTB).

Three types of palaeomagnetic procedures were applied: conventional archaeodirection and archaeointensity determinations (at the Palaeomagnetic Laboratory of Barcelona, SCT UB-CSIC); and microwave archaeointensity determinations (at the Geomagnetism Laboratory, University of Liverpool). Archaeodirectional analyses consisted of stepwise demagnetization of the natural remanent magnetization (NRM) and measurement of the magnetization left after each step. Thermal demagnetization was performed in a Schoenstedt TSD-1 demagnetizer and magnetization measurements on a 2G Enterprises superconducting rock magnetometer. Results were presented as Zijderveld diagrams (Zijderveld, 1967). Characteristic remanent magnetization (ChRM) directions were calculated by principal component analyses (Kirschvink, 1980). Three anomalous directions were obtained (one per kiln), possibly due to an incorrect replacement of broken cylinders during sampling. These outliers were removed from the calculation of mean directions. Mean directions for each kiln and merged mean directions were computed following Fisher (1953) statistics; concentration parameter k and confidence factor α_{95} were also computed. The mean direction was compared with i) the SVC for the Iberian Peninsula (Gómez-Paccard et al., 2006) and ii) SCHA.DIF.3K model (Pavón-Carrasco et al., 2009) predictions using a Matlab dating tool developed by Pavón-Carrasco et al. (2011). The Iberian SVC is defined at a central location (Madrid) and it was computed by the hierarchical Bayesian method using archaeomagnetic directions with dates ranging from 775 BC to 1959 AD. The SCHA.DIF.3K model was obtained by least-sums of absolute deviation inversion of palaeomagnetic data using spherical harmonics (SCHA) and provides full geomagnetic field vector values over the European continent and neighbouring areas from 1000 BC to 1900 AD.

Archaeointensity analyses were performed according to the Coe variant of a Thellier-type experiment (Coe, 1967), the NRM was measured and gradually removed and replaced by a new thermal magnetization (TRM). This was achieved by heating the samples alternatively in a zero (Z) and a 50 μT applied (A) field in a Magnetic Measurements MMTD-80 thermal demagnetizer. Besides the conventional Z/A steps, pTRM and pTRM tail checks (Riisager and Riisager, 2001) were performed to ensure the absence of alteration and multidomain behaviour within the magnetic remanence carriers. The remanent magnetization measurements were also performed on a 2G Enterprises superconducting rock magnetometer. Cooling rate tests were performed at 560 °C on all samples following the procedure described in Chauvin et al. (2000). The correction was applied only for samples with stable acquisition capacity ($r_2 < 5\%$ where $r_2 = (TRM_1 - TRM_3)/TRM_1$). Microwave archaeointensity analyses followed a similar procedure, although using microwaves instead of heat to directly generate magnons (Shaw et al., 1999) to erase the NRM or to generate a new microwave thermoremanent magnetization (T_MRM). The microwave system used operated in the 14 GHz frequency range; throughout the experiments the frequency was finely tuned to the ferromagnetic resonant frequency of the sample and after irradiation allowed direct measurement of the magnetization. Both conventional and microwave archaeointensity results were represented as Arai plots where NRM lost is plotted against TRM (or T_MRM) gained, both normalized to the initial NRM along with the pTRM and tail checks (Yu and Dunlop, 2003). Additionally Zijderveld diagrams were also plotted using the steps performed in zero field to check the directional uniformity of the NRM vector. An overall archaeointensity value was computed for each kiln by fitting a Gaussian function to the sum of all individual results (Fouzai et al., 2012). Samples with negative pTRM checks or *f* values lower than 0.5 (Biggin and Thomas, 2003) were not used to obtain the overall intensity estimate. Positive pTRM checks were defined as those with a difference between the original pTRM and the pTRM check lower than 10 percent of the total TRM acquired (Chauvin et al., 2000).

Table 1
Sampled features in El Vila-sec (Latitude: 41.24°N, Longitude: 1.17°E) with indication of their presumed ages according to archaeological evidence, the sample labels, the number of collected cores (*N*) and the applied archaeomagnetic technique.

Kiln	Presumed age	Label	*N*	Technique
7	50 BC–50 AD	K7	23[a]	Conventional archaeointensity
9	50 AD–225 AD	K9	5	Conventional archaeodirection
11	50 AD–150 AD	K11	9	Conventional archaeodirection
12	50 AD–150 AD	K12	9	Conventional archaeodirection
12	50 AD–150 AD	K12	3	Microwave archaeointensity

[a] From 3 quadrangular bricks.

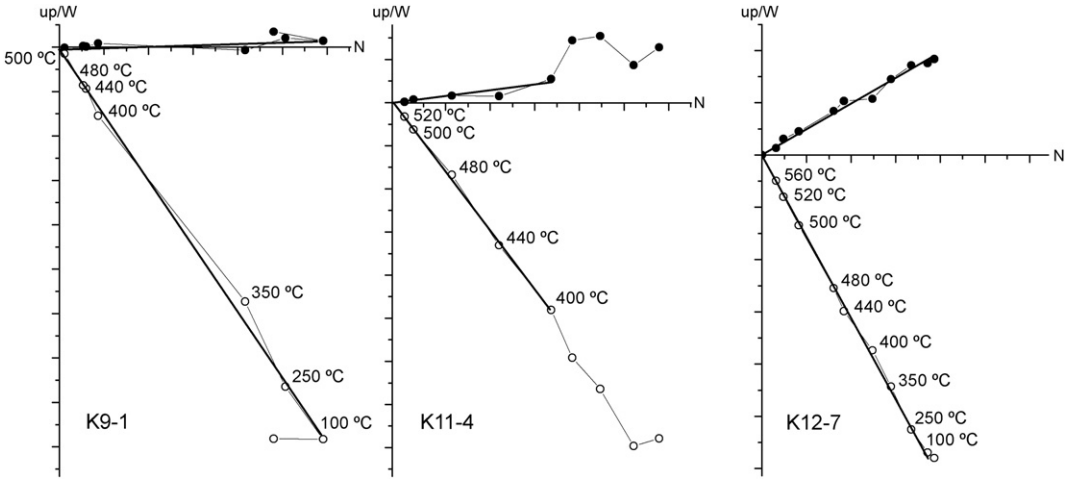

Fig. 10. Representative Zijderveld plots depicting the orthogonal projection of the remanent magnetization vectors during progressive demagnetization for specimens from Kiln 9 (left), Kiln 11 (middle) and Kiln 12 (right). Open (solid) symbols represent projections on vertical (horizontal) planes. Lines indicate the ChRM directions.

The full archaeomagnetic vector (including both mean direction and intensity) was also compared with the previously described SCHA.DIF.3K model. The use of an archaeomagnetic field model avoids the need for relocation of data to a central location, a procedure that involves an inherent error (Casas and Incoronato, 2007). However, the use of archaeomagnetic field models involves regularization and smoothing to interpolate field values, which can also be a source of error.

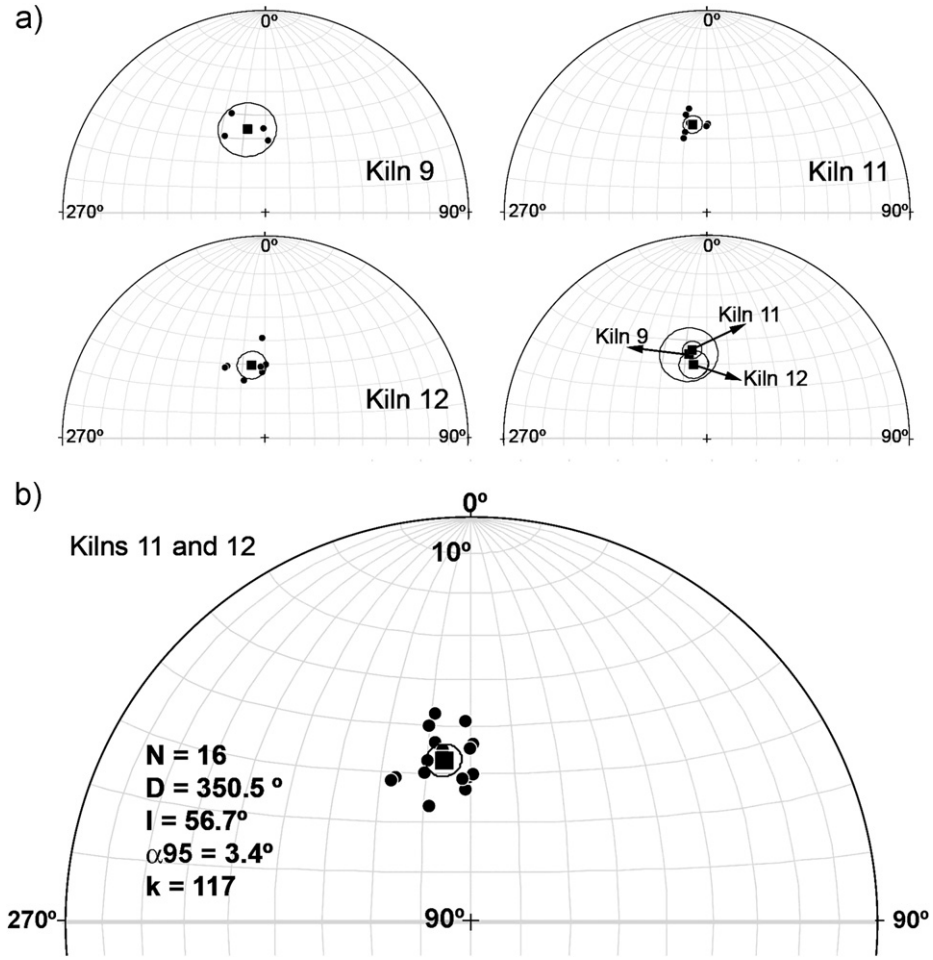

Fig. 11. Stereographic projection of the archaeomagnetic directions calculated for each sample. In (a) mean directions and α_{95} error circles were calculated and plotted separately for each kiln, in (b) the individual results from the Kilns 11 and 12 were merged to produce a single mean direction and α_{95} error. *N* indicates the total number of samples from the two kilns; *D* and *I* stands for declination and inclination; α_{95} and *k*, 95% confidence cone of the mean direction and precision parameter from Fisher statistics.

4. Results and discussion

4.1. The mean archaeomagnetic vector

Representative Zijderveld diagrams of samples from Kilns 9, 11 and 12 are shown in Fig. 10. Usually almost all the temperature steps were taken into account to compute the ChRM directions. MAD values were always lower than 5. The obtained archaeodirections were plotted separately for each kiln in stereographic projections (Fig. 11a). The three kilns produce slightly different mean directions (Table 2), possibly due to the low number of samples per kiln (four from Kiln 9, eight each from Kilns 11 and 12). Archaeological evidence indicates that the three kilns are practically contemporary. Taking into account the sampled points, the results from Kilns 11 and 12 can be ascribed to a very constrained age (the second archaeological phase), whereas the four results from Kiln 9 could correspond either to the second or the third archaeological phase. Adding this to the fact that Kiln 9 only produced four scattered directions, it is reasonable to combine the archaeodirections from Kilns 11 and 12 to produce a single mean direction (Fig. 11b and Table 2) expressed as a declination of 350.5° and an inclination of 56.7° ($\alpha_{95} = 3.4°$) that according to the archaeological evidence would correspond to a narrow time window (mid-1st century AD to mid-2nd century AD).

Archaeointensity determinations based on a constant proportionality between remanence magnetization and magnetic field is known to be limited to stable non-interacting single domain (SD) or pseudo-single domain (PSD) remanence carriers (Fabian, 2001). Using the magnetization parameters and coercitive field (from the hysteresis loops) and the remanence coercivity (from a backfield experiment) the Day plots revealed that all the measured cores can be attributed to the PSD regime. However, temperature-dependent susceptibility measurements indicate that six cores do contain MD particles: the appearance of a characteristic peak (Fig. 12a) around 130 K (the Verwey transition) indicates low-Ti titanomagnetite in MD state (Moskowitz, 1980). In fact, the PSD field in a Day plot can also be ascribed to a mixture of SD and multidomain (MD) states (Dunlop, 2002). Magnetization versus temperature curves indicate a distribution of blocking temperatures for all analyzed cores. This could be due either to a broad distribution of magnetic particle sizes or to a distribution of Ti contents within the titanomagnetites of the analyzed core. The degree of thermal reversibility after heating at 700 °C is variable (Fig. 12b); the darker materials tend to show a loss of magnetic signal after heating, whereas for the brownish materials the trend is towards increased magnetic signal. The decrease in signal can be related to oxidation reactions. The increase in magnetic signal could relate to the growth of magnetic grains through agglomeration.

Archaeointensity specimens obtained from the same cores that exhibit hints of MD behaviour were not analyzed. Representative Arai diagrams of specimens from Kilns 7 and 12 with the corresponding Zijderveld diagrams are shown in Fig. 13. A total of 31 specimens were analyzed (eighteen from Kiln 7 and thirteen from Kiln 12), only three exhibit non linear Arai plots (one from Kiln 7 and two from Kiln 12). The rest of specimens are listed in Table 3 (Kiln 7) and Table 4 (Kiln 12) with the corresponding archaeointensities. Only one specimen from the Kiln 7 set was rejected due to negative pTRM checks, whereas three were rejected for this reason from the Kiln 12 set, and two other K12 specimens were rejected due to low f fractions. Fig. 14 shows the overall archaeointensity results for each kiln (71.39 ± 14.27 μT for Kiln 7 and 70.11 ± 7.00 μT for Kiln 12). Thus, despite being measured with different techniques and although the two kilns are not exactly contemporary according to the archaeological evidence, both show virtually identical archaeointensities. This agrees with the SCHA.DIF.3K predictions of a low rate of intensity variations for the first five centuries AD. From the two archaeointensities, the value obtained for Kiln 12 can be directly linked to the obtained mean direction to date the second archaeological phase.

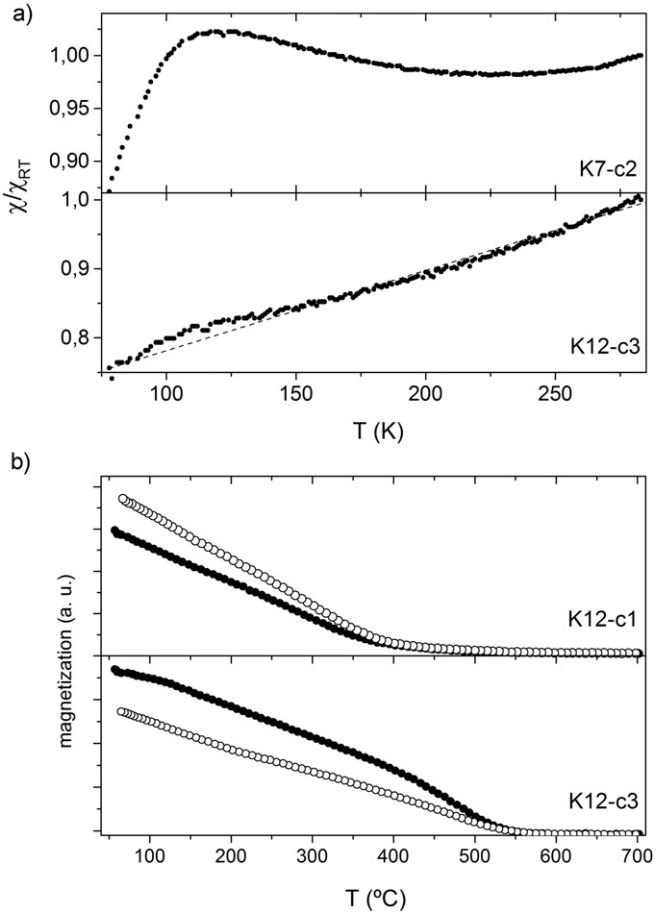

Fig. 12. (a) Low temperature susceptibility dependence for samples from Kilns 7 (top) and 12 (bottom) exhibiting hints of the Verwey transition. (b) Thermomagnetic curves for samples from Kiln 12 exhibiting an increase (top) or decrease (bottom) of the magnetic signal after heating at 700 °C.

Table 2
Archaeomagnetic directional results.

Kiln	n/N	D (°)	I (°)	k	α_{95} (°)
9	4/4	347.8	55.3	67.9	11.2
11	8/8	351.1	53.5	229.9	3.7
12	8/8	349.9	59.9	95.7	5.7
All	20/20	350.0	56.4	109.0	3.1
11 and 12	16/16	350.5	56.7	117.2	3.4

Columns from left to right: Kiln, number of the sampled kiln; n/N, number of specimens analyzed (n)/independently oriented samples taken into account in the calculation of the mean direction (N); k and α_{95}, precision parameter and 95% confidence limit of characteristic remanent magnetization, from Fisher statistics.

4.2. Archaeomagnetic dating tools

The archaeomagnetic results ascribed to the second archaeological phase were used to check the proficiency of the available archaeomagnetic dating tools. Probability density functions of possible dates for declination and inclination were obtained comparing the relocated data with the Iberian SVC. Both functions were then combined to obtain the most probable

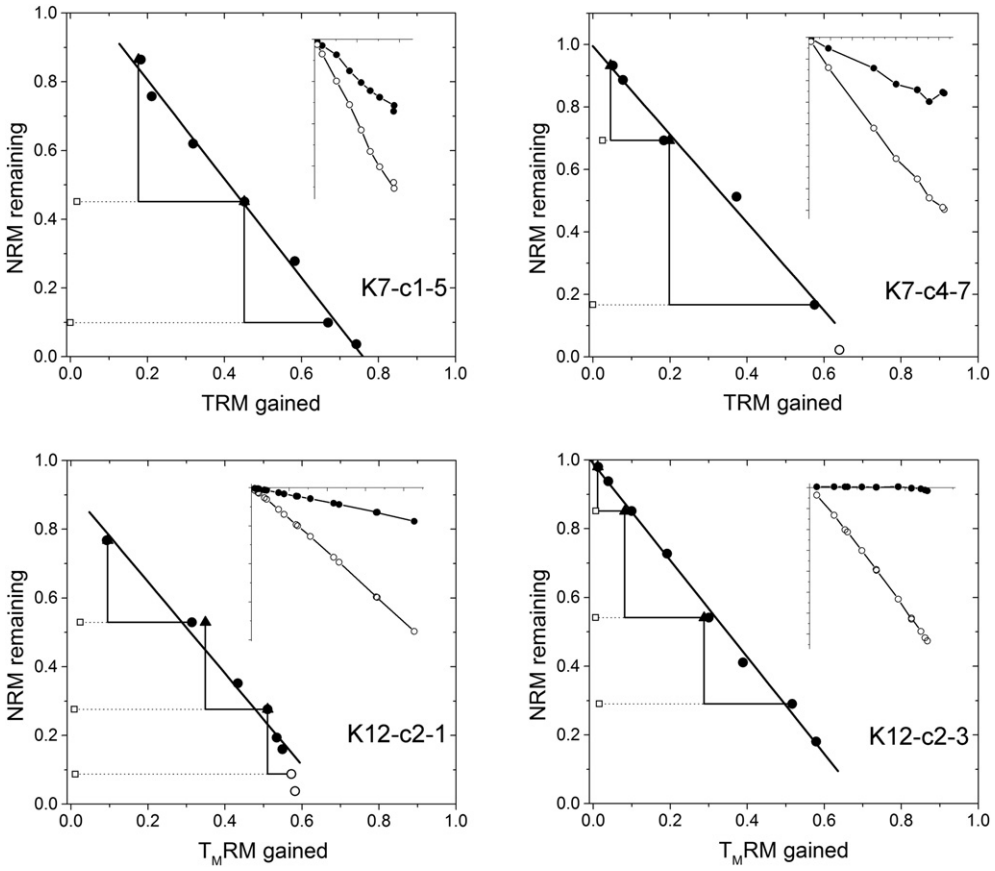

Fig. 13. Representative Arai plots of normalized NRM remaining against TRM (or T_MRM) gained for specimens from Kilns 7 and 12. The corresponding Zijderveld diagrams are plotted in the upper right corner of each Arai plot.

solution at 95% confidence level. The procedure is illustrated in Fig. 15. The combined (declination and inclination) probability distribution is split in three intervals (BC 203–132, BC 23–AD 507 and AD 1836–1900). The presumed archaeological age (AD 50–150) lies within the wider interval and concentrates about 15% of the obtained probability distribution (Fig. 15). The third interval would indicate a modern remagnetization of the studied structures. The same described procedure was applied to the non-relocated data using the SCHA.DIF.3K model. The corresponding probability distributions are shown in Fig. 16. The combined probability distribution presents similar features when compared to the distribution obtained using the SVC: it is split

Table 3
Conventional archaeomagnetic intensity results for Kiln 7 obtained from linear Arai plots. All specimens except K7-c21 (negative pTRM checks) were used to compute the mean intensity value.

Brick	Specimen	F (μT)	F_{CR} (μT)	σ (μT)	N	f	g	q
1	K7-c1	72.13	68.67	3.90	7	0.83	0.82	18.5
1	K7-c3	84.21	74.39	7.84	5	0.65	0.68	10.7
1	K7-c4	70.78	–	8.06	5	0.77	0.67	8.8
1	K7-c5	83.46	76.47	21.34	4	0.52	0.51	3.9
1	K7-c6	85.47	–	5.22	4	0.80	0.62	16.4
1	K7-c7	71.83	–	5.89	4	0.65	0.62	12.2
2	K7-c8	60.17	–	16.98	5	0.52	0.44	3.5
2	K7-c9	64.46	56.64	10.30	7	0.69	0.78	6.3
2	K7-c10	55.64	51.60	10.70	6	0.75	0.77	5.2
2	K7-c11	85.12	76.64	18.40	5	0.74	0.50	4.6
2	K7-c12	84.53	–	2.71	5	0.74	0.66	31.2
2	K7-c13	74.72	–	5.11	3	0.68	0.44	14.6
2	K7-c14	64.59	–	52.6	3	0.65	0.48	1.2
3	K7-c20	58.42	–	19.2	4	0.58	0.55	3.0
3	K7-c21	83.13	–	16.9	5	0.74	0.50	4.9
3	K7-c22	80.80	80.38	16.9	5	0.50	0.74	4.8
3	K7-c23	58.43	–	6.2	4	0.50	0.62	9.5
Mean value		71.39 ± 14.27						

Columns from left to right: Brick, label identifying the brick provenance; Specimen, label of the specimen identifying the kiln (K7) and the core number; F, raw intensity; F_{CR}, cooling rate corrected intensity; σ, standard deviation of the intensity estimate; N, number of heating steps used for the intensity determination; f, fraction of NRM used for intensity determination; g, gap factor and q, quality factor as defined by Coe (1967).

Table 4
Microwave archaeomagnetic intensity results for Kiln 12 obtained from linear Arai plots.

Specimen	F (μT)	σ (μT)	N	f	g	q	pTRM
K12-c1-1	65.52	3.48	6	0.53	0.70	18.85	✓
K12-c1-2	66.51	21.00	4	0.72	0.63	3.2	×
K12-c1-3	68.37	7.32	6	0.57	0.71	9.3	✓
K12-c1-4	71.91	6.95	5	0.55	0.53	10.4	✓
K12-c1-5	53.86	11.09	4	0.55	0.54	4.9	×
K12-c1-6	51.23	4.27	4	0.51	0.48	12.0	×
K12-c2-1	67.02	9.00	5	0.61	0.69	7.5	✓
K12-c2-2	71.26	173.53	3	0.18	0.46	0.4	–
K12-c2-3	70.53	2.74	8	0.80	0.84	25.7	✓
K12-c2–4	78.58	4.24	6	0.64	0.69	18.5	✓
K12-c2-5	72.54	27.78	4	0.32	0.64	2.6	–
Mean value	71.11 ± 7.00						

Columns from left to right: Specimen, label of the specimen identifying the kiln (K12), the core number and the specimen; F, intensity; σ, standard deviation of the intensity estimate; N, number of heating steps used for the intensity determination; f, fraction of NRM used for intensity determination; g, gap factor and q, quality factor as defined by Coe (1967); pTRM, result of the pTRM check test: passed (✓), failed (✓) or not performed (–).

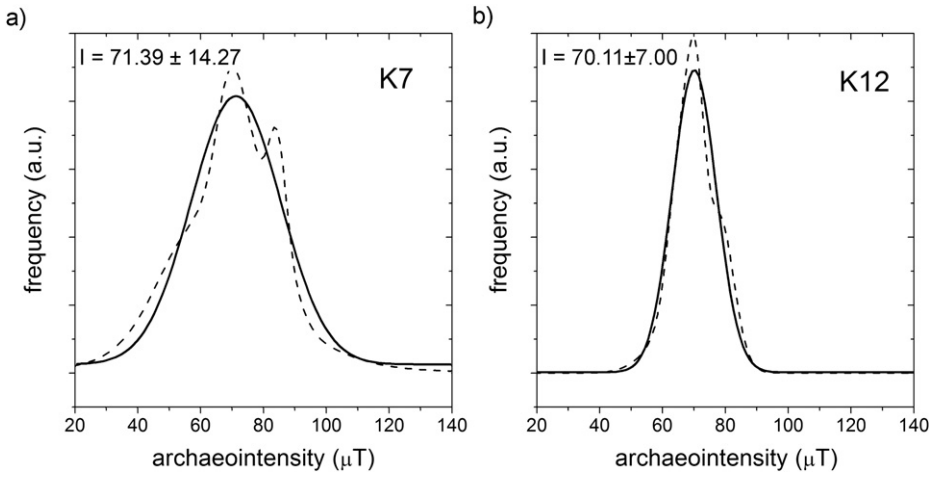

Fig. 14. Computation of mean archaeointensities for Kilns 7 (a) and 12 (b). The dashed line is the sum of all the accepted individual archaeointensity results for the kiln and the solid line is a Gaussian fitting to those sums.

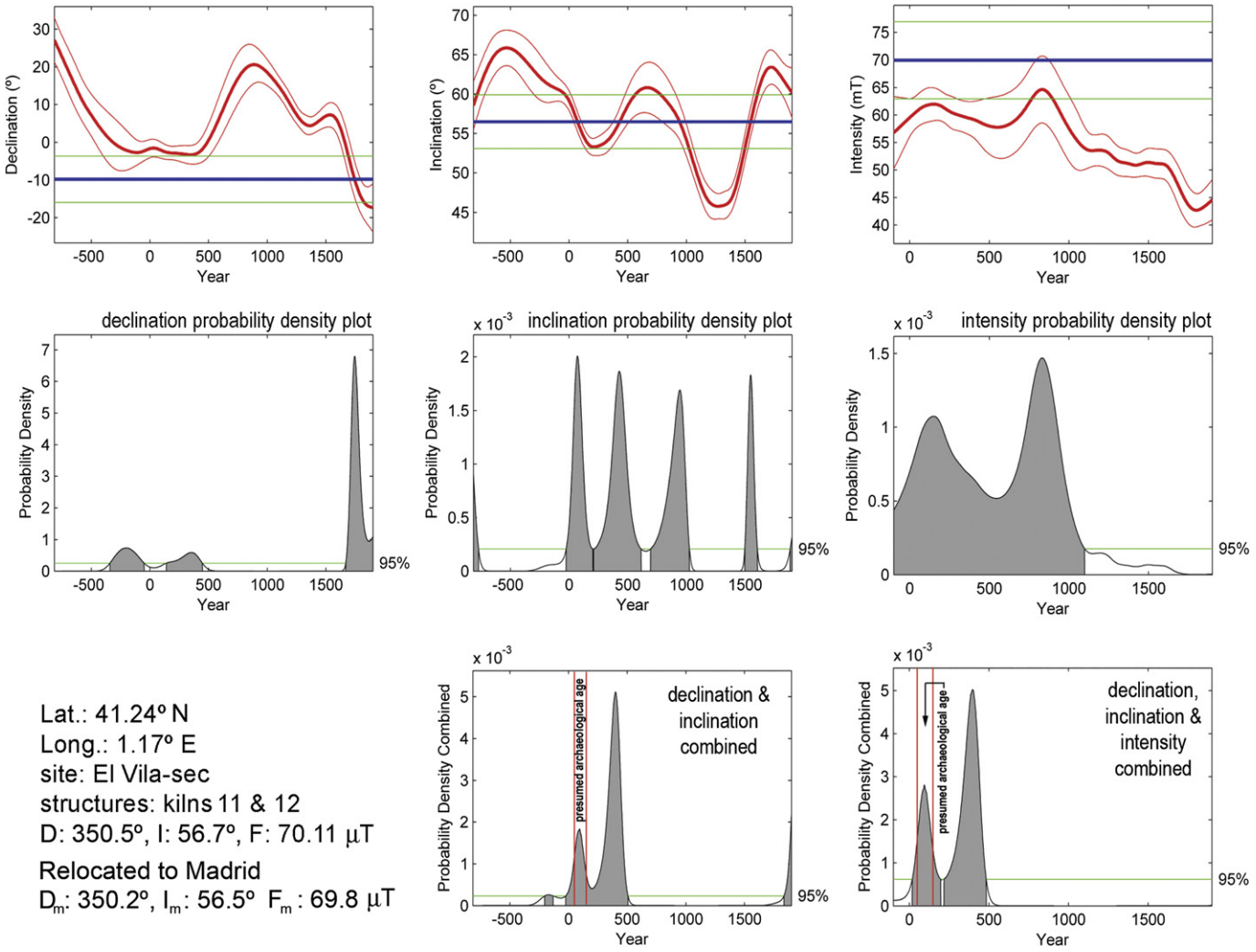

Fig. 15. Probability-of-age density functions obtained with the Matlab tool from Pavón-Carrasco et al. (2011) comparing the Iberian SVC with the merged archaeodirectional results from Kilns 11 and 12 relocated to Madrid; relocated intensity results from Kiln 12 were compared with the Bayesian SVC for western Europe. At the bottom: location of the site, experimental archaeomagnetic vector probability function without intensity data (middle) and including them (right).

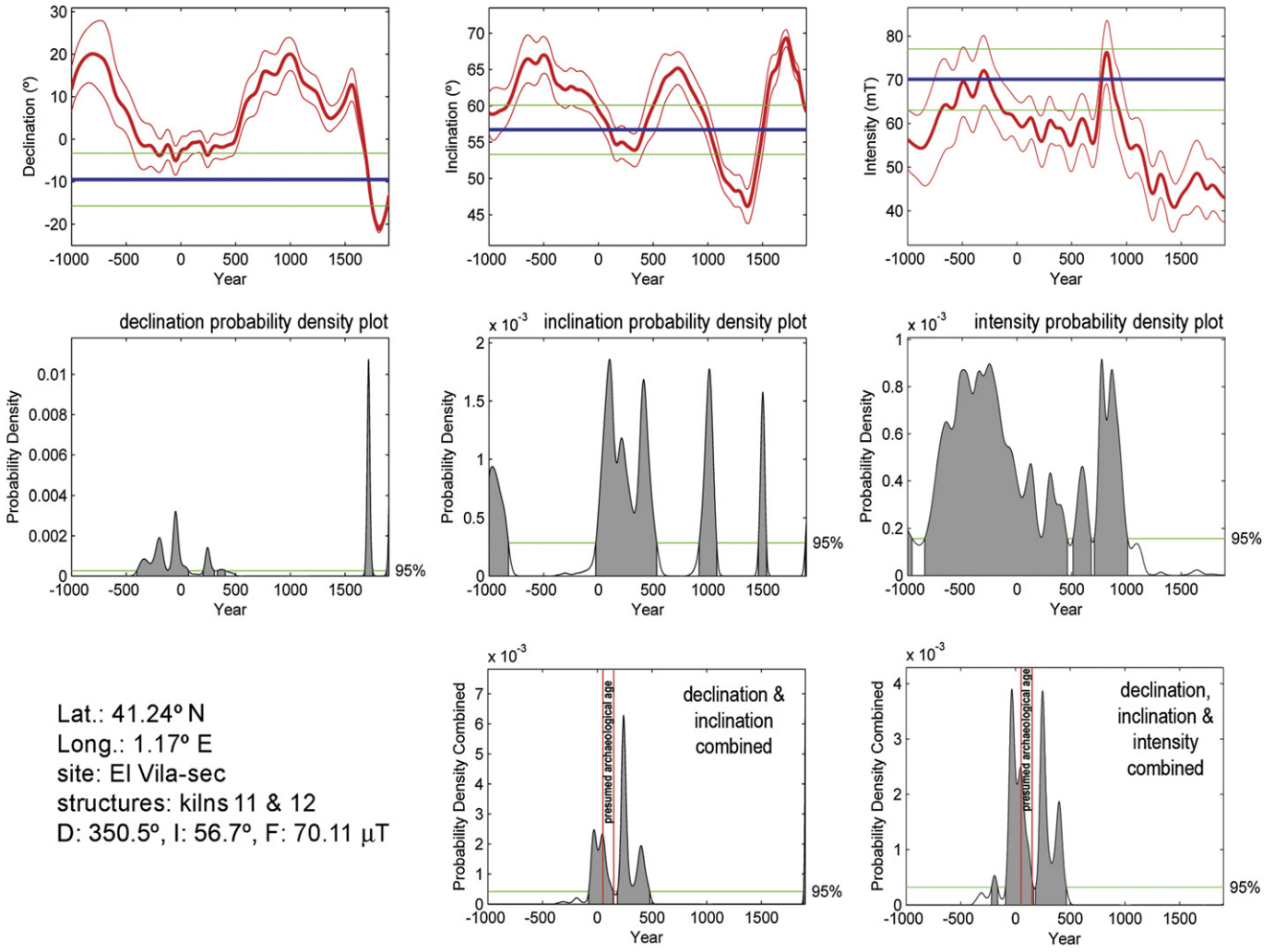

Fig. 16. Probability-of-age density functions obtained with the Matlab tool from Pavón-Carrasco et al. (2011) comparing the SCHA.DIF.3K model predictions with the archaeomagnetic results (the merged archaeodirectional results from Kilns 11 and 12, and the archaeointensity from Kiln 12). At the bottom: location of the site, experimental archaeomagnetic vector and probability function without intensity data (middle) and including them (right).

into three time intervals, the first (BC 79–AD 145) includes the presumed archaeological age, the second (AD 184–479) concentrates a significant amount of probability and the third points to a modern remagnetization (AD 1886–1900). In this case, the presumed archaeological time window represents 10% of the obtained probability distribution. The main difference from the SVC-obtained distribution is that the SCHA.DIF.3K-obtained distribution contains more ups and downs; this dissimilarity reflects the difference between the wiggled SCHA.DIF.3K model curves and the more smoothed Iberian SVC.

Table 5
Archaeomagnetic dating results.

Kiln	Input	Dating tool	Main solutions at 95% confidence level. (in bold letters the solution that matches with the PAA)	Presumed archaeological age (PAA)	% of probability within the PAA
K7	Intensity	SCHA.DIF.3K	**BC 1000–AD 1202** AD 1279–1350 AD 1580–1703	BC 50–AD 50	5
K11 + K12	Direction (relocated)	Iberian SVC	BC 203–132 **AD 23–507 AD** AD 1836–1900	AD 50–150	15
	Direction + intensity (relocated)	Iberian SVC + western European intensity SVC	**AD 19–197** AD 218–483		22
	Direction	SCHA.DIF.3K	**BC 79–145 AD** AD 184–479 AD 1885–1900		13
	Direction + intensity	SCHA.DIF.3K	BC 226–159 **BC 93–AD 167** AD 182–464		15

The intensity data can be also added to the dating procedure, the Iberian SVC only predicts the evolution of the archaeomagnetic direction and therefore the Bayesian SVC for western Europe (Gómez-Paccard et al., 2008) has been used for the relocated data. In contrast, the SCHA.DIF.3K simulates the full archaeomagnetic vector. Despite its large error, it is worth mentioning that the contribution of the archaeointensity data helped to constraint the possible ages. Both, the probability distributions obtained combining the direction data with either the Iberian SVC (adding the western European intensity SVC) or the SCHA.DIF.3K include a time interval pointing to a modern remagnetization. The geomagnetic field strength is presently around 45 μT, far below the measured archaeointensities for Kiln 12 and thus, adding the intensity to the dating procedure, the modern magnetization hypothesis can be excluded. The fully combined (declination, inclination and intensity) probability distribution results in an increased concentration of probability within the presumed archaeological time window: using the Iberian SVC (adding the western European intensity SVC) the time window contains 22% of the probability (Fig. 15); using the SCHA.DIF.3K model the time window concentrates 15% of the probability (Fig. 16). Table 5 summarizes the dating results obtained.

The measured archaeointensity for Kiln 7 alone (without the corresponding directional data) cannot provide information on its archaeomagnetic age because the probability distribution covers almost the full investigated time period (see Table 5).

The archaeointensities obtained for Kilns 7 and 12 are significantly higher than the model predictions. This result was also found for Roman sites in Tunisia (Fouzai et al., 2012) and seems to suggest that during this period the intensity is not well resolved by the model due to a limited intensity database.

5. Conclusions

A highly precise dating for the activity at the Vila-sec Roman pottery workshop was determined using the typology of its ceramic materials. A chronology of three different phases was established. A first phase with seven kilns that were abandoned in the middle of the 1st century AD, a second with four kilns active from the middle of the 1st century AD to the middle of the 2nd century AD and a third with three kilns (two of them rebuilt from second-phase kilns) active up until the late 2nd or early 3rd century AD.

Structures from the first archaeological phase could not be precisely dated by archaeomagnetic methods because of the major uncertainty associated with the mean archaeointensity and the lack of archaeodirectional data for Kiln 7. The age of the second archaeological phase was checked with three archaeomagnetic dating tools. Both the Iberian SVC and the SCHA.DIF.3K models have a similar level of accuracy. Nevertheless, the SCHA.DIF.3K model has the advantage of not requiring data relocation and also predicts archaeointensities, which in this case allowed a modern remagnetization to be ruled out. Combining the western European intensity SVC with the Iberian SVC also allowed, using relocated data, a modern remagnetization to be ruled out. Furthermore this combination resulted in the highest concentration of probability within the presumed archaeological age (22%). In any case, none of the archaeomagnetic dating approaches produced a single unambiguous solution pointing to the presumed archaeological age. We have to keep in mind that a given value of the archaeomagnetic vector can occur at different time periods. Besides that, secular variation curves and geomagnetic models are not foolproof and only a continuous effort to collect reliable archaeomagnetic data from well-dated structures will increase their accuracy.

Archaeointensities of almost contemporary structures were determined by two different techniques (microwave and the conventional Thellier method) and yielded similar results. This again suggests that T_MRM and TRM are equivalent (Shaw et al., 1999; Hill et al., 2002; Casas et al., 2005). The obtained archaeointensities seem to imply that during this period the intensity is not well resolved by the SCHA.DIF.3K model, due to a limited intensity database. This reinforces the conclusion that the collection of reliable archaeomagnetic data from well-dated structures is required.

Only with high quality data, can the archaeomagnetic approaches undertaken be applied to dating other archaeological sites from the same region, particularly when they lack any datable artefacts.

Acknowledgements

We would like to thank Elisabeth Schnepp for her helpful and insightful comments. This research was funded by the Spanish Ministerio de Ciencia e Innovación (Project HAR2010-16953) and the Agencia Española de Cooperación Internacional para el Desarrollo (Spain-Tunisia bilateral project A1/039844/11).

References

Aitken, M.J., 1974. Physics and Archaeology. Clarendon Press, Oxford.
Berni Millet, P., 2010. Epigrafia sobre *amphorae*, *tegulae*, *imbrex* i *dolia* a l'àrea occidental del Camp de Tarragona (Epigraphy on amphorae, tegulae, imbrex and dolia in the western area of the Camp of Tarragona). In: Gorostidi, D. (Ed.), Ager Tarraconensis 3. Les inscripcions romanes/The Roman Inscriptions. Institut Català d'Arqueologia Clàssica, Tarragona, pp. 153–210. Documenta 16.
Berni Millet, P., 2011. Nota sobre un nou segell ANT-VEN de la producció amfòrica de Mas d'en Corts (Reus, Baix Camp). In: Prevosti, M., Guitart i Duran, J. (Eds.), Ager Tarraconensis 2. El poblament/The Population. Institut Català d'Arqueologia Clàssica, Tarragona, pp. 490–495. Documenta 16.
Biggin, A.J., Thomas, D.N., 2003. The application of acceptance criteria to results of Thellier palaeointensity experiments performed on samples with pseudo-single-domain-like characteristics. Physics of the Earth and Planetary Interiors 138, 279–287.
Berti, F., Carandini, A., Fabbricotti, E., 1970. Ostia II. Le terme del Nuotatore. Scavo dell'ambiente I, Studi Miscellanei 16. Roma.
Casas, Ll, Incoronato, A., 2007. Distribution analysis of errors due to relocation of geomagnetic data using the 'Conversion via Pole' (CVP) method: implications on archaeomagnetic data. Geophysical Journal International 169, 448–454.
Casas, Ll., Shaw, J., Gich, M., Share, J.A., 2005. High-quality microwave archaeointensity determinations from an early 18th century AD English brick kiln. Geophysical Journal International 161, 653–661.
Casas, Ll., Briansó, J.L., Álvarez, A., Benzzi, K., Shaw, J., 2008. Archaeomagnetic intensity data from the Saadien Tombs (Marrakech, Morocco), late 16th century. Physics and Chemistry of the Earth, Parts A/B/C 33, 474–480.
Catanzariti, G., Gómez-Paccard, M., McIntosh, G., Pavón-Carrasco, F.J., Chauvin, A., Osete, M.L., 2012. New archaeomagnetic data recovered from the study of Roman and Visigothic remains from central Spain (3rd–7th centuries). Geophysical Journal International 188, 979–993.
Chauvin, A., Garcia, Y., Lanos, P., Laubenheimer, F., 2000. Paleointensity of the geomagnetic field recovered on archaeomagnetic sites from France. Physics of the Earth and Planetary Interiors 120, 111–136.
Coe, R.S., 1967. Paleo-intensities of Earth's magnetic field determined from Tertiary and Quaternary rocks. Journal of Geophysical Research 72, 3247–3262.
Cuomo di Caprio, N., 1971. Proposta di classificazione delle fornaci per ceramica e laterizi nell'area italiana. Sibrium, pp. 371–464.
Cuomo di Caprio, N., 1985. La Ceramica in archeologia: antiche tecniche di lavorazione e moderni metodi d'indagine. "L'Erma" di Bretschneider, Roma.
Cuomo di Caprio, N., 2007. La ceramica in archeologia, 2: antiche tecniche di lavorazione e moderni metodi di indagine. "L'Erma" di Bretschneider, Roma.
Dragendorff, H., 1895. Terra Sigillata. Ein Beitrag zur Geschichte der griechischen und römischen Keramik, vol. 96. Bonner Jahrbücher, Bonn, pp. 18–155.
Dressel, H., 1899a. Amphorae. Inscriptiones Vrbis Romae Latinae. Instrumentum domesticum, Corpus Inscriptionum Latinarum XV/2, p. 1.
Dressel, H., 1899b. Lucernae, Inscriptiones Vrbis Romae Latinae. Instrumentum domesticum, Corpus Inscriptionum Latinarum XV/2, p. 1.
Dunlop, D.J., 2002. Theory and application of the Day plot (M-rs/M-s versus H-cr/H-c) 1. Theoretical curves and tests using titanomagnetite data. Journal of Geophysical Research-Solid Earth 107, 2056.
Ettlinger, E., Hedinger, B., Hoffmann, B., Kenrick, Ph.M., Pucci, G., Roth-Rubi, K., Schneider, G., Schnurbein, S. von, Wells, C.M., Zabehlicky-Scheffenegger, S., 1990. Conspectus formarum terrae sigillatae italico modo confectae. Dr. Rudolf Habelt GMBH, Bonn.

Fabian, K., 2001. A theoretical treatment of paleointensity determination experiments on rocks containing pseudo-single or multi domain magnetic particles. Earth and Planetary Science Letters 188, 45–58.
Fisher, R., 1953. Dispersion on a sphere. Proceedings of the Royal Society of London, Series A. Mathematical and Physical Sciences 217, 295–305.
Fouzai, B., Casas, Ll., Laridhi Ouazaa, N., Álvarez, A., 2012. Archaeomagnetic data from four Roman sites in Tunisia. Journal of Archaeological Science 39, 1871–1882.
Genin, M. (Ed.), 2007. La Graufesenque (Millau, Aveyron). Sigillées lisses et autres productions, vol. II. Éditions de la Fédération Aquitania, Études d'archéologie urbaine, Pessac.
Gómez-Paccard, M., Beamud, E., 2008. Recent achievements in archaeomagnetic dating in the Iberian Peninsula: application to Roman and Mediaeval Spanish structures. Journal of Archaeological Science 35, 1389–1398.
Gómez-Paccard, M., Chauvin, A., Lanos, P., McIntosh, G., Osete, M.L., Catanzariti, G., Ruiz-Martínez, V.C., Núñez, J.I., 2006. First archaeomagnetic secular variation curve for the Iberian Peninsula: comparison with other data from Western Europe and with global geomagnetic field models. Geochemistry, Geophysics, Geosystems 7, Q12001.
Gómez-Paccard, M., Chauvin, A., Lanos, Ph., Thiriot, J., 2008. New archeointensity data from Spain and the geomagnetic dipole moment in Western Europe over the past 2000 years. Journal of Geophysical Research 113, B09103. http://dx.doi.org/10.1029/2008JB005582.
Hayes, J.W., 1972. Late Roman Pottery. The British School at Rome, London.
Hill, M.J., Gratton, M.N., Shaw, J., 2002. A comparison of thermal and microwave palaeomagnetic techniques using lava containing laboratory induced remanence. Geophysical Journal International 151, 157–163.
Járrega, R., Otiña, P., 2008. Un tipo de ánfora tarraconense de época medioimperial (siglos II-III): la Dressel 2–4 evolucionada. SFECAG, Actes du Congrès de L'Escala-Empúries, pp. 281–286.
Járrega, R., Prevosti, M., 2011. Figlinae tarraconenses. La producció ceràmica a l'ager Tarraconensis. In: Prevosti, M., Guitart i Duran, J. (Eds.), Ager Tarraconensis 2. El poblament/The Population. Institut Català d'Arqueologia Clàssica, Tarragona, pp. 455–490. Documenta 16.
Kirschvink, J.L., 1980. The least-squares line and plane and the analysis of paleomagnetic data. Geophysical Journal of the Royal Astronomical Society 62, 699–718.
Lamboglia, N., 1958. Nuove osservazioni sulla terra sigillata chiara (tipi A e B). Rivista di Studi Liguri 24, 257–330. Bordighera.
Le Goff, M., Gallet, Y., Genevey, A., Warmé, N., 2002. On archeomagnetic secular variation curves and archeomagnetic dating. Physics of the Earth and Planetary Interiors 134, 203–211.
López Mullor, A., 1989. Las cerámicas romanas de paredes finas en Cataluña, Quaderns científics i tècnics. Diputació de Barcelona, Barcelona (2 vols.).
López Mullor, A., Aquilué, X. (Eds.), 2008. La producció i el comerç de les àmfores de la Província Hispania Tarraconensis. Homenatge a Ricard Pascual i Guasch, vol. 8. Monografies del Museu d'Arqueologia de Catalunya, Barcelona.
López Mullor, A., Martín, A., 2008. Tipologia i datació de les àmfores tarraconenses produïdes a Catalunya. In: López Mullor, A., Aquilué, X. (Eds.), La producció i el comerç de les àmfores de la Província Hispania Tarraconensis. Homenatge a Ricard Pascual i Guasch, vol. 8. Monografies del Museu d'Arqueologia de Catalunya, Barcelona, pp. 33–94.
Mayet, F., 1975. Les céramiques à parois fines dans la Péninsule Ibérique. Publication du Centre Pierre Paris, CNRS, Paris.
Mezquíriz, M.A., 1961. Terra Sigillata Hispànica. The William L. Bryant Foundation, Valencia.
Mezquíriz, M.A., 1985. Terra sigillata hispànica. In: VV.AA, et al. (Eds.), Atlante delle forme ceramiche II. Ceramica fine romana nel bacino mediterraneo (tardo ellenismo e primo Impero). Enciclopedia dell'Arte Antica Classica e Orientale, pp. 97–174. Roma.
Morillo Cerdán, A., 1989. En torno a la tipología de lucernas: Problemas de nomenclatura. Cuadernos de Prehistoria y Arqueología 17, 143–167. Universidad Complutense de Madrid.
Moskowitz, B.M., 1980. Theoretical grain-size limits for single-domain, pseudo-single-domain and multi-domain behavior in titanomagnetite (X = 0.6) as a function of low-temperature oxidation. Earth and Planetary Science Letters 47, 285–293.
Oswald, F., Pryce, T.D., 1920. An Introduction to the Study of Terra Sigillata. Treated from a Chronological Standpoint. Longmans, Green, and Co., London.
Pascual, R., 1977. Las ánforas de la Layetania, Méthodes classiques et méthodes formelles dans l'étude des amphores. Collection de l'École Française de Rome, Roma, pp. 47–96.
Passelac, M., Vernhet, A., 1993. Céramique sigillée sud-gauloise. In: [DICOCER] (Ed.), Dictionaire des Céramiques Antiques (VIIème s. av. n. è. – VIIème s. d. n. è.) en Mediterranée nord-occidentale (Provence, Languedoc, Ampurdan), Lattara, vol. 6, pp. 569–580. Edisud, Lattes.
Pavolini, C., 1987. Le lucerne romane fra il III sec. AC e il III sec. dC, Céramiques hellenistiques et romaines, II. París, pp. 139–166.
Pavón-Carrasco, F.J., Osete, M.L., Torta, J.M., Gaya-Pique, L.R., 2009. A regional archeomagnetic model for Europe for the last 3000 years, SCHA.DIF.3K: applications to archeomagnetic dating. Geochemistry, Geophysics, Geosystems 10, Q03013.
Pavón-Carrasco, F.J., Rodriguez-Gonzalez, J., Osete, M.L., Torta, J.M., 2011. A Matlab tool for archaeomagnetic dating. Journal of Archaeological Science 38, 408–419.
Prevosti, M., 2009. L'arqueologia del vi a l'àrea costanera de la Tarraconense. Una reflexió. In: Prevosti, M., Martín i Oliveras, A. (Eds.), El vi tarraconense i laietà: ahir i avui. Actes del simpòsium. Institut Català d'Arqueologia Clàssica, Tarragona, pp. 249–259. Documenta 7.
Prevosti, M., Guitart i Duran, J. (Eds.), 2011. Ager Tarraconensis 2. El poblament/The population. Institut Català d'Arqueologia Clàssica, Tarragona. Documenta 16.
Prevosti, M., Guitart i Duran, J. (Eds.), 2010. Ager Tarraconensis 1. Ager Tarraconensis 1. Aspectes històrics i marc natural/Historical Aspects and Natural Setting. Institut Català d'Arqueologia Clàssica, Tarragona. Documenta 16.
Prevosti, M., Martín i Oliveras, A. (Eds.), 2009. El vi tarraconense i laietà: ahir i avui. Actes del simpòsium. Institut Català d'Arqueologia Clàssica, Tarragona. Documenta 7.
Raynaud, Cl., 1993a. Amphores de Bétique. In: [DICOCER] (Ed.), Dictionaire des Céramiques Antiques (VIIème s. av. n. è. – VIIème s. d. n. è.) en Mediterranée nord-occidentale (Provence, Languedoc, Ampurdan), Lattara, vol. 6, pp. 23–27. Edisud, Lattes.
Raynaud, Cl., 1993b. Céramique africaine Claire A. In: [DICOCER] (Ed.), Dictionaire des Céramiques Antiques (VIIème s. av. n. è. – VIIème s. d. n. è.) en Mediterranée nord occidentale (Provence, Languedoc, Ampurdan), Lattara, vol. 6, pp. 170–174. Edisud, Lattes.
Raynaud, Cl, 1993c. Céramique africaine de cuisine. In: DICOCER (Ed.), Dictionaire des Céramiques Antiques (VIIème s. av. n. è. – VIIème s. d. n. è.) en Mediterranée nord occidentale (Provence, Languedoc, Ampurdan), Lattara, vol. 6, pp. 87–89. Edisud, Lattes.
Riisager, P., Riisager, J., 2001. Detecting multidomain magnetic grains in Thellier palaeointensity experiments. Physics of the Earth and Planetary Interiors 125, 111–117.
Ritterling, E., 1913. Das frührömische Lager bei Hofheim im Taunus. Annalen des Vereins für Nassauische Altertumskunde 40. Wiesbaden.
Roca, M., Fernández García, M.I. (Eds.), 2005. Introducción al estudio de la cerámica romana. Una breve guía de referencia. Servicio de Publicaciones de la Universidad de Málaga, Málaga.
Roig, J.F., 2007. Darreres evidències d'època romana a l'actual terme d'Alcover: el camí del Molí i el Vila-sec. Butlletí del Centre d'Estudis Alcoverencs 114, 45–60.
Roig, J.F., 2008. El jaciment arqueològic del Vila-sec: el material ceràmic. Butlletí del Centre d'Estudis Alcoverencs 115, 67–83.
Roig, J.F., 2009. La bòbila romana del Vila-sec: els forns ceràmics. Butlletí del Centre d'Estudis Alcoverencs 116, 44–64.
Roig, J.F., 2010. Memòria de la intervenció arqueològica al jaciment del Vila-sec afectat per les obres de l'eix Alcover-Reus (C-14), (Alcover, Alt Camp). CODEX, Unpublished report, Arxiu del Servei d'Arqueologia del Departament de Cultura de la Generalitat de Catalunya, Tarragona.
Schnepp, E., Lanos, P., Chauvin, A., 2009. Geomagnetic paleointensity between 1300 and 1750 A.D. derived from a bread oven floor sequence in Lübeck, Germany. Geochemistry, Geophysics, Geosystems 10, Q08003. http://dx.doi.org/10.1029/2009GC002470.
Sciallano, M., Sibella, P., 1993. Amphores – comment les identifier? Lattara 6. Edisud, Lattes.
Shaw, J., Yang, S., Rolph, T.C., Sun, F.Y., 1999. A comparison of archaeointensity results from Chinese ceramics using microwave and conventional Thellier's and Shaw's methods. Geophysical Journal International 136, 714–718.
Yu, Y.J., Dunlop, D.J., 2003. On partial thermoremanent magnetization tail checks in Thellier paleointensity determination. Journal of Geophysical Research – Solid Earth 108, 2523.
Zananiri, I., Batt, C.M., Lanos, P., Tarling, D.H., Linford, P., 2007. Archaeomagnetic secular variation in the UK during the past 4000 years and its application to archaeomagnetic dating. Physics of the Earth and Planetary Interiors 160, 97–107.
Zijderveld, J.D.A., 1967. Natural remanent magnetizations of Exeter volcanic traps (Permian Europe). Tectonophysics 4, 121–153.